

# Bulletin of the Seismological Society of America

## PROBABILISTIC FAULT DISPLACEMENT HAZARD ASSESSMENT (PFDHA) FOR NUCLEAR INSTALLATIONS ACCORDING TO IAEA SAFETY STANDARDS

--Manuscript Draft--

<b>Manuscript Number:</b>	BSSA-D-21-00083R2
<b>Article Type:</b>	Article
<b>Section/Category:</b>	Special Section - Fault Displacement and Near-Source Ground Motion Models
<b>Full Title:</b>	PROBABILISTIC FAULT DISPLACEMENT HAZARD ASSESSMENT (PFDHA) FOR NUCLEAR INSTALLATIONS ACCORDING TO IAEA SAFETY STANDARDS
<b>Corresponding Author:</b>	Alessandro Valentini, Ph.D International Atomic Energy Agency Vienna, AUSTRIA
<b>Corresponding Author's Institution:</b>	International Atomic Energy Agency
<b>Corresponding Author E-Mail:</b>	alessandro.valentini@unich.it
<b>Order of Authors:</b>	Alessandro Valentini, Ph.D Yoshimitsu Fukushima Paolo Contri Masato Ono Toshiaki Sakai Stephen Thompson Emmanuel Viallet Tadashi Annaka Rui Chen Robb Moss Mark Petersen Francesco Visini Robert Youngs
<b>Abstract:</b>	<p>In the last ten years, the International Atomic Energy Agency (IAEA) revised its safety standards for site evaluations of nuclear installations in response to emerging fault displacement hazard evaluation practices developed in Member States. New amendments in the revised safety guidance (DS507) explicitly recommend fault displacement hazard assessment, including separate approaches for candidate new sites versus existing sites. If there is insufficient basis to conclusively determine that a fault is not capable of surface displacement at an existing site, then a probabilistic fault displacement hazard analysis (PFDHA) is recommended to better characterize the hazard. This new recommendation has generated the need for the IAEA to provide its Member States with guidance on performing PFDHA, including its formulation and implementation. This paper provides an overview of current PFDHA state-of-practice for nuclear installations that is consistent with the new IAEA safety standards. We also summarize progress in an on-going international PFDHA benchmark project that will ultimately provide technical guidance to Member States for conducting site-specific fault displacement hazard assessments.</p>
<b>Author Comments:</b>	All comments included in the decision letter has been addressed.
<b>Suggested Reviewers:</b>	Stephane Baize stephane.baize@irsn.fr Shigekazu Kusumoto kusu@bep.vgs.kyoto-u.ac.jp

	Ivan Wong wong@lettisci.com
	Naoto Inoue naoto@geor.or.jp
	Yousef Bozorgnia yousefbozorgnia@g.ucla.edu
<b>Opposed Reviewers:</b>	
<b>Response to Reviewers:</b>	
<b>Additional Information:</b>	
<b>Question</b>	<b>Response</b>
<p><b>Key Point #1:</b> Three key points will be printed at the front of your manuscript so readers can get a quick overview. Please provide three COMPLETE sentences addressing the following: 1) state the problem you are addressing in a FULL sentence; 2) state your main conclusion(s) in a FULL sentence; and 3) state the broader implications of your findings in a FULL sentence. Each point must be 110 characters or less (including spaces).</p>	<p>We describe a benchmarking project born from a request of the Member States to provide more examples on PFDHA</p>
<b>Key Point #2:</b>	Base case and sensitivity cases results show high variability in terms of hazard curves
<b>Key Point #3:</b>	The benchmarking project will deliver a document which will assist the Member States in performing PFDHA

1     **PROBABILISTIC FAULT DISPLACEMENT HAZARD ASSESSMENT (PFDHA) FOR**  
2             **NUCLEAR INSTALLATIONS ACCORDING TO IAEA SAFETY STANDARDS**

3  
4     Alessandro Valentini\*<sup>1</sup> Yoshimitsu Fukushima<sup>1</sup> Paolo Contri<sup>1</sup> Masato Ono<sup>1</sup> Toshiaki Sakai<sup>2</sup>  
5     Stephen C. Thompson<sup>3</sup> Emmanuel Viallet<sup>4</sup> Tadashi Annaka<sup>5</sup> Rui Chen<sup>6</sup> Robb E. S. Moss<sup>7</sup> Mark  
6             D. Petersen<sup>8</sup> Francesco Visini<sup>9</sup> Robert R. Youngs<sup>10</sup>

7  
8             <sup>1</sup> International Atomic Energy Agency, IAEA, Vienna, Austria

9             <sup>2</sup> Central Research Institute of Electric Power Industry, Abiko, Japan

10            <sup>3</sup> Lettis Consultants International, Inc., Concord, California, USA

11            <sup>4</sup> Électricité de France, Technical Direction, Lyon, France

12            <sup>5</sup> Tokyo Electric Power Services Company, Ltd., Tokyo, Japan

13            <sup>6</sup> California Geological Survey, Sacramento, California, USA

14     <sup>7</sup> Department Civil and Environmental Engineering, Cal Poly, San Luis Obispo, California, USA

15            <sup>8</sup> U.S. Geological Survey, Denver, Colorado, USA

16            <sup>9</sup> Istituto Nazionale di Geofisica e Vulcanologia, Sezione di Pisa, Italy

17            <sup>10</sup> Wood Environment & Infrastructure Solutions, Inc. Oakland, California, USA

18  
19  
20     \*Corresponding author:

21     Alessandro Valentini

22     External Events Safety Section

23     International Atomic Energy Agency, IAEA

24 Vienna International Centre, PO Box 100

25 1400 Vienna, Austria

26 A.Valentini@iaea.org

27

28  
29  
30  
31  
32  
33  
34  
35  
36  
37  
38  
39  
40  
41  
42  
43  
44  
45  
46  
47  
48  
49  
50

## ABSTRACT

In the last ten years, the International Atomic Energy Agency (IAEA) revised its safety standards for site evaluations of nuclear installations in response to emerging fault displacement hazard evaluation practices developed in Member States. New amendments in the revised safety guidance (DS507) explicitly recommend fault displacement hazard assessment, including separate approaches for candidate new sites versus existing sites. If there is insufficient basis to conclusively determine that a fault is not capable of surface displacement at an existing site, then a probabilistic fault displacement hazard analysis (PFDHA) is recommended to better characterize the hazard. This new recommendation has generated the need for the IAEA to provide its Member States with guidance on performing PFDHA, including its formulation and implementation. This paper provides an overview of current PFDHA state-of-practice for nuclear installations that is consistent with the new IAEA safety standards. We also summarize progress in an on-going international PFDHA benchmark project that will ultimately provide technical guidance to Member States for conducting site-specific fault displacement hazard assessments.

*Keywords: capable faults, probabilistic fault displacement hazard analysis, nuclear installations*

## INTRODUCTION

The International Atomic Energy Agency (IAEA) establishes “International Safety Standards” through a consensus process among Member States (i.e., all States that have joined the International Atomic Energy Agency) to ensure nuclear safety and security worldwide. The

51 IAEA's Safety Standards Series consists of three elements: (i) Safety Fundamentals, (ii) Safety  
52 Requirements, and (iii) Safety Guides (Fig. 1). The Safety Fundamentals, which constitute the  
53 basis of the Standards, provide ten principles associated with the fundamental safety objective of  
54 protecting people and the environment from harmful effects of ionizing radiation (IAEA, 2006).  
55 To embody these principles, Safety Requirements are defined whereas the subordinate Safety  
56 Guides provide technical recommendations and guidelines to meet the Safety Requirements.  
57 Safety Guides are published with consensus from all IAEA Member States and provide high-level  
58 recommendations on how to meet the Safety Requirements. Safety Reports and Technical  
59 Documents (TECDOC series) provide specific technical guidance on the state-of-practice that can  
60 be applied to meet the recommendations in the Safety Guides (Fig. 1).

61         Fault displacement hazards for nuclear installations are addressed in the IAEA Safety  
62 Fundamentals (IAEA, 2006), Safety Requirements (IAEA, 2019), and Safety Guides (IAEA, 2010  
63 and IAEA, 2021a). Safety Principle 8 ("Prevention of Accidents") in the current Safety  
64 Fundamentals (IAEA, 2006) pertains to fault displacement hazards, stating that all practical efforts  
65 must be made to prevent and mitigate nuclear accidents, and the suitability and selection of a site  
66 must be evaluated considering the effects of external events, site characteristics, and environment  
67 (IAEA, 2006). Safety Requirement No. SSR-1 (IAEA, 2019) outlines 29 requirements a site shall  
68 satisfy to support Safety Principle 8. Requirement 15 ("Evaluation of fault capability") in SSR-1  
69 (IAEA, 2019) concerns fault displacement hazards, mandating faults within a certain distance of  
70 the site that are important to safety shall be identified, and fault displacement hazards shall be  
71 evaluated if a fault is identified as capable (i.e., it has a significant potential for displacement at or  
72 near the ground surface). Safety Guide No. SSG-9 (IAEA, 2010) provides high-level  
73 recommendations that a site should meet to comply with Safety Principle 8 and the requirements

74 in SSR-1. This 2010 Safety Guide (SSG-9) will be superseded by DS507 (IAEA, 2021a).  
75 Currently, there is one TECDOC that directly addresses fault displacement hazard analysis by  
76 giving an introduction and overview of PFDHA and examples of its application in some Member  
77 States (IAEA, 2021b).

78 Probabilistic analysis is recommended for fault displacement hazard evaluations in Safety  
79 Guide SSG-9 at existing nuclear sites if a capable fault is identified within the site vicinity (5 km  
80 radius) (IAEA, 2010). While the existence of a capable fault within 5 km of a candidate site is  
81 considered an exclusionary criterion for new nuclear installations under SSG-9, new data can  
82 emerge after a nuclear installation is operational. Recognizing the importance of systematically  
83 evaluating new data, SSG-9 recommends that fault displacement hazards should be evaluated  
84 using a probabilistic approach (i.e., PFDHA) if a newly identified fault has the potential to affect  
85 the safety of an existing nuclear installation, and that the evaluation should determine whether the  
86 expected displacement value would exceed a permissible displacement value (IAEA, 2010).

87 The IAEA's recommendation to use probabilistic approaches to evaluate fault  
88 displacement hazards is based on experience and regulations developed in United States, Japan,  
89 and other Member States. For example, the American National Standards Institute (ANSI)  
90 provides criteria and guidelines for assessing tectonic ground deformation and surface fault rupture  
91 for nuclear facilities (Standard ANSI-ANS-2.30, 2015). Similar to the IAEA's SSG-9 Safety Guide  
92 (IAEA, 2010), the ANSI-ANS-2.30 guidelines state that any known Quaternary fault (within 5  
93 km) shall be evaluated for potential displacement hazards at the site. Per ANSI-ANS-2.30, the  
94 PFDHA evaluation may be performed in accordance with the Senior Seismic Hazard Analysis  
95 Committee's (SSHAC) principles developed for ground shaking probabilistic seismic hazard  
96 assessments (United States Nuclear Regulatory Commission, 2018). The Atomic Energy Society

97 of Japan (AESJ) is also updating a standard procedure for probabilistic fault displacement risk  
98 assessment (The Standards Committee of AESJ, 2021).

99         The currently available documents and guidelines that recommend the use of PFDHA for  
100 nuclear installations do so at a high level, without details on the methodology or its implementation  
101 (IAEA 2010, 2021a, 2021b, and ANSI-ANS-2.30, 2015). The publication of only one, introductory  
102 TECDOC on the topic reflects the facts that PFDHA is relatively new and its practice uncommon.  
103 Example applications of PFDHA for nuclear installations are limited, and the related information  
104 is largely inaccessible to the Member States. Accordingly, the IAEA Member States expressed a  
105 desire to receive more practical guidance on PFDHA during the 14th Plenary Meeting, ‘Technical  
106 Meeting on Protection of Nuclear Installations Against External Hazards’, held in November 2020  
107 in Vienna. Member States requested specific examples of PFDHA implementation through a new  
108 benchmarking exercise that could be documented in a TECDOC. The intent of the new  
109 benchmarking exercise is to provide a comparison of current methodologies and uncertainties. It  
110 will provide state-of-the-practice documentation to support Member States in their implementation  
111 of PFDHA at their nuclear installation sites, and allow Member States to conduct PFDHA at  
112 existing and/or new nuclear installations following the recommendation of SSG-9 (IAEA, 2010)  
113 and DS507 (IAEA, 2021a) and fulfilling the requirements of SSR-1 (IAEA, 2019).

114         In this paper, we provide an overview of the state-of-practice of PFDHA for nuclear  
115 installations and introduce the IAEA PFDHA Benchmarking Project. The project is an on-going  
116 international effort led by the IAEA, and preliminary results consisting of a base case for hazard  
117 calculation and model verification are documented herein. We also discuss sensitivity cases to  
118 explore how PFDHA models perform under different site-fault configurations, and remaining tasks  
119 in the benchmarking project are described.



120

121 **PROBABILISTIC FAULT DISPLACEMENT HAZARD ASSESSMENT FOR NUCLEAR**

122

**INSTALLATIONS**

123

124 In Safety Requirement No. SSR-1 (IAEA, 2019), a fault is considered capable if,  
125 considering all available geological, geophysical, geomorphological, geodetic, and seismological  
126 data, one of the following conditions is satisfied: i) it shows evidence of past surface deformations  
127 and/or dislocations of a recurring nature, from which it can be inferred that future surface  
128 deformations could occur; ii) there is a structural relationship with a known capable fault, and  
129 movement of one could cause movement of the other, yielding ruptures at or near the surface; and  
130 iii) it is possible to infer, from the tectonic setting of the site and the maximum potential earthquake  
131 of the seismogenic structure, that movement at or near the surface could occur. In areas of high  
132 seismic activity where the earthquake recurrence intervals are relatively short, capable faults may  
133 be assessed by evaluating evidence for activity over time periods on the order of tens of thousands  
134 of years. In contrast, a much longer time period may be required in less tectonically active areas  
135 to better evaluate fault activity and assess the capability of a fault to produce surface-rupturing  
136 earthquakes.

137 IAEA Safety Guides SSG-9 (IAEA, 2010) and DS507 (IAEA, 2021a) differentiate primary  
138 (i.e., principle) and secondary (i.e., distributed) faults for fault displacement hazard assessment  
139 and provide siting recommendations based on the distinction. Primary fault ruptures occur along  
140 a fault rupture plane (or planes) from which seismic energy is released, whereas secondary fault  
141 ruptures occur near the primary rupture on associated faults such as splays or branches of the  
142 capable fault, or antithetic structures (Coppersmith and Youngs, 2000; Youngs et al., 2003; IAEA,

143 2021b). Safety Guide SSG-9 recommends that new nuclear installation sites be located at least 5  
144 km from any capable fault that could potentially affect the safety of the installation, unless the  
145 effects can be compensated by proven engineering design or other protective measures (i.e.,  
146 exclusionary criterion). If any capable fault is identified within 5 km of an existing nuclear  
147 installation, SSG-9 recommends conducting PFDHA. Safety Guide DS507 updates these criteria  
148 for both new and existing sites, considering if the capable fault is classified as primary or  
149 secondary.

150 Fig. 2 illustrates candidate (new) site selection criteria per DS507 (IAEA, 2021a). Two  
151 cases are shown: (a) secondary faults are identified within the site area, and the capable primary  
152 fault is within the site vicinity; and (b) secondary faults are within the site vicinity, but the capable  
153 primary fault is outside the site vicinity. According to DS507, case (a) should be a basis for  
154 excluding the candidate site if the effects of secondary fault ruptures cannot be compensated by  
155 any proven engineering design or other protective measures, whereas in case (b), selection of the  
156 candidate site remains at the discretion of the Member States' regulatory bodies. Per DS507, if a  
157 fault cannot be classified as primary or secondary, then the fault should be characterized as primary  
158 to be conservative. Both cases (a) and (b) were considered exclusionary criteria for new sites in  
159 Safety Guide SSG-9 (IAEA, 2010), which does not distinguish between primary and secondary  
160 fault rupture. The new distinction between primary and secondary fault ruptures in DS507  
161 encourages Member States to perform detailed geological surveys for better characterization of  
162 faults in the vicinity of a nuclear installation.

163 New nuclear installations can avoid known capable faults. While detailed site  
164 investigations are required before the construction of a nuclear installation, new information can  
165 later be acquired that identify a capable fault. When capable faults are discovered near existing

166 sites, the hazard needs to be assessed to identify potential safety issues. In this case, a PFDHA  
167 should be performed, per SSG-9 and DS507, to estimate the annual frequencies of exceedance for  
168 primary and secondary displacement values of interests at or near the surface. Assessments can be  
169 performed following the approaches described in the next section and should address epistemic  
170 uncertainty adequately, as recommended by the IAEA Safety Standard.

171 The IAEA exclusionary and discretionary criteria are summarized in Figure 2 for new sites  
172 and in Table 1 for new and existing nuclear installations. For new installations, Cases 1 and 2 are  
173 exclusionary criteria, but Case 3 is a discretionary criterion. For an existing nuclear installation, if  
174 the fault has a potential to affect the safety of the nuclear installation, PFDHA evaluations are  
175 recommended for Cases 1 and 2. There currently is no recommendation for Case 3.

176 Only three PFDHA nuclear installation case studies have been performed for IAEA  
177 Member States in the past 20 years with documentation of the uncertainties and limitations in the  
178 approaches used. These studies are: 1) the Yucca Mountain nuclear waste repository in Nevada,  
179 USA, 2) the Diablo Canyon nuclear power plant in California, USA, and 3) a planned additional  
180 power plant adjacent to the existing Krško nuclear power plant in Slovenia (IAEA, 2021b). A  
181 description of these three case studies and details about their approaches are given in the IAEA  
182 TECDOC ‘An Introduction to Probabilistic Fault Displacement Hazard Analysis in Site Evaluation  
183 for Existing Nuclear Installations’ (IAEA, 2021b).

184

## 185 **OVERVIEW OF PFDHA METHODOLOGY**

186

187 PFDHA aims to provide the likelihood of occurrence of various amounts of coseismic  
188 surface-fault displacement. The pioneering publication of Youngs et al. (2003) presented two

189 approaches: an earthquake approach and a displacement approach. They provided  
190 parameterizations of the earthquake approach suitable for normal faulting environments. The  
191 earthquake approach was developed utilizing the well-developed probabilistic seismic hazard  
192 analysis (PSHA) framework for ground motion hazards. It relies on magnitude-recurrence  
193 relationship to derive the rate of exceedance for various amounts of displacement at a site on or  
194 near a fault. The displacement approach, in contrast, uses direct observations of past fault  
195 displacement at a site to constrain and quantify the relationship between exceedance frequency  
196 and displacement amount.

197 Subsequently, several groups proposed different approaches for different tectonic  
198 environments. Petersen et al. (2011) developed an earthquake approach and provided regression  
199 equations for both principal and distributed displacement on strike-slip faults, using their  
200 compilation of historical surface displacement data. Moss and Ross (2011) presented a similar  
201 earthquake approach and provided data and equations for principal displacement on reverse faults.  
202 Takao et al. (2013) provided data and regressions for strike-slip and reverse faults in Japan. More  
203 recently, Lavrentiadis and Abrahamson (2019) developed a wavenumber-domain methodology to  
204 capture the correlation of the surface-slip variability along a strike, avoid the surface-rupture length  
205 normalization, and narrow tails of the slip distribution, which is important for PFDHA at long  
206 return periods. Nurminen et al. (2020) developed a model for distributed displacement hazard for  
207 reverse faults and introduced a novel statistical approach to estimate the conditional probability of  
208 distributed ruptures as a function of distance from the principal fault.

209 In any PFDHA, the first step consists of seismic source identification and characterization  
210 to determine earthquake frequency and distance distributions, followed by calculating the annual  
211 frequency ( $\lambda$ ) for fault displacement  $D$  exceeding  $D_0$  (IAEA, 2021b):

212

$$\lambda(D > D_0) = \alpha_{DE} \cdot P(D > D_0) \quad (1)$$

214

215 where  $\alpha_{DE}$  is the rate of displacement events at the site and  $P(D > D_0)$  is the probability that  
216 displacement  $D$  exceeds the threshold level  $D_0$ . Eq. 1 is applicable to both primary and secondary  
217 displacements. Depending on whether there are data at or near the site of interest to quantify  $\alpha_{DE}$   
218 and the exceedance probability distribution  $P(D > D_0)$ , the displacement or earthquake approach  
219 can be followed.

220

### 221 ***Earthquake Approach***

222

223 The earthquake approach formulation is similar to that for PSHA (Cornell, 1968), and uses  
224 an integration over a set of earthquake scenarios distributed on the fault. The simple event rate  $\alpha_{DE}$   
225 in Eq. 1 is replaced with the overall rate of events  $\alpha(m_{min})$  with magnitudes larger than a given  
226 minimum magnitude ( $m_{min}$ ) and a probability density function  $f_{m,s}$  that describes the magnitude  $m$   
227 earthquake, occurring along an active fault at distance  $s$  from the end of the fault, as follows (IAEA,  
228 2021b):

229

$$\alpha_{DE} = \alpha(m_{min}) \int f_{m,s}(m, s) dm ds \quad (2)$$

231

232 Following this approach, the probabilistic term in Eq. 1 becomes an attenuation function  
233 for fault displacement at or near the ground surface and it contains two parts (Eq. 3):

234

235 
$$P(D > D_0) = P[D \neq 0 | z, r, sr \neq 0] \times P[D > D_0 | l/L, m, D \neq 0] \quad (3)$$

236

237 The former part is the conditional probability that fault displacement exceeds  $D_0$  at the site  
 238 given slip occurs ( $D \neq 0$ ). The latter represents the probability of having surface slip at distance  $r$   
 239 from the fault rupture, over an area  $z^2$ , with a magnitude  $m$  event that ruptures the surface.  $l/L$  is  
 240 along-fault distance ratio, where  $L$  is the total rupture length and  $l$  is the distance from the nearest  
 241 point on the fault rupture to the closest end of the rupture.

242 Not all earthquakes break the surface, depending on the magnitude of the earthquake, an  
 243 additional magnitude-dependent term (Eq. 4) must be considered in Eq. 1 in order to define the  
 244 probability that a fault produces surface rupture:

245

246 
$$P[sr \neq 0 | m] \quad (4)$$

247

248 Moreover, a probability density function,  $f_r(r)$ , describing the perpendicular distance from  
 249 the site to all potential ruptures is also incorporated. Combining Eqs. 2 through Eq. 4 and  
 250 integrating over magnitudes and location distributions, Eq. 1 can be written as follows (IAEA,  
 251 2021b):

252

253 
$$\lambda(D > D_0) = \alpha(m_{\min}) \int f_{m,s} P[sr \neq 0 | m] \times \quad (5)$$
  

$$\times \int P[D \neq 0 | z, r, sr \neq 0] \times P[D > D_0 | l/L, m, D \neq 0] f_r(r) dm ds dr$$

254

255 This general form applies to principal faulting. Depending on seismotectonic setting and  
 256 available data, this general form can contain additional details or variables introduced by model

257 developers. For example, Takao et al. (2013) considered an additional conditional probability term  
258 to account for the observation that the ratio of surface and subsurface rupture lengths depends on  
259 magnitude. The general form of Eq. 5 can also be applied to distributed faulting by replacing the  
260 distance ratio  $l/L$  with the distance  $r$  between the principal fault and the site of interest. Several  
261 models are available to assess distributed faulting (Youngs et al., 2003; Petersen et al., 2011; Takao  
262 et al, 2013; Nurminen et al., 2020).

263

### 264 *Displacement Approach*

265

266 Developed as a part of the Yucca Mountain study (Stepp et al., 2001; Youngs et al. 2003),  
267 the displacement approach utilizes only the observations and characteristics of fault displacement  
268 at the point of interest to assess the hazard. Unlike the earthquake approach, there is no distinction  
269 between principal and distributed faulting, and the causative source is not explicitly considered.  
270 The rate of exceedance  $\nu$  for a given level of displacement  $d$  can be obtained by the general form:

271

$$272 \quad \nu(d) = \lambda_{DE} \cdot P(D > d) \quad (6)$$

273

274 where  $\lambda_{DE}$  is the rate of displacement events and  $P(D > d)$  is the conditional probability, given a  
275 slip on the fault, that the single-event displacement  $D$  will exceed the value  $d$ .

276 The rate of displacement  $\lambda_{DE}$  can be estimated from the slip rate  $SR$  and the average slip  $D_E$   
277 in a faulting event ( $\lambda_{DE} = SR/D_E$ ) or directly from the recurrence intervals  $R_{int}$  of paleoearthquake  
278 age ( $\lambda_{DE} = 1/R_{int}$ ). The probability term in Eq. 6 can be estimated from a database of repeated slip

279 events revealed at the same location or using generic distributions for normalized displacement  
280 along with an estimate of the average displacement.

281

## 282 **IAEA PFDHA BENCHMARKING PROJECT**

283

284 The objective of the IAEA PFDHA Benchmarking Project is to provide information on the  
285 state-of-practice and detailed technical elements related to PFDHA to assist Member States in  
286 implementing the recommendations of SSG-9 and DS507 for evaluation of fault displacement  
287 hazards at existing and/or new nuclear installations. Special attention is devoted to benchmarking  
288 available PFDHA models via scenario case studies, identifying necessary model refinements at  
289 individual sites, and discussion of evaluating uncertainty.

290 The benchmarking study consists of a simple verification exercise, calculating hazards for  
291 a straightforward set of test cases. The study consists of three steps: 1) verification of current  
292 published models and model comparison; 2) model implementation for two sites; and 3)  
293 documentation of the model verification, comparison, and test case implementation in an IAEA  
294 TECDOC. The project officially started in November 2020 and its expected duration is two years.

295 Step 1 includes a simple fictional scenario with a single seismic source parameterization  
296 and a logic tree capturing epistemic uncertainty in source parameterization. Although a range of  
297 scenarios is considered in a full PFDHA, we considered only specific scenarios because this is a  
298 benchmarking exercise. The goals of the first step are: i) to engage the PFDHA model developers  
299 and have them provide mean hazard curves, ii) to establish “baseline” hazard curves for later  
300 verification exercises, and iii) to analyse results to guide activities for the second step. The fictional  
301 scenarios and logic tree inputs for seismic sources were provided by the IAEA. In particular, the



302 IAEA provided site coordinates and site dimensions in Excel and Esri shapefile format, and source  
303 characterization logic trees. The lead modelers who participated in Step 1 are: R. Youngs (for  
304 Youngs et al., 2003), R. Chen (for Petersen et al., 2011), R. Moss (for Moss and Ross, 2011 and  
305 2013), T. Annaka (for Takao et al., 2013, 2014, and 2016), and F. Visini (for Nurminen et al.,  
306 2020). They and other participants provided results as tables, plots, and short answers to questions  
307 about their approaches.

308         Whereas Step 1 only included only developers of currently published PFDHA models, Step  
309 2 will expand to include other teams with experience in implementing PFDHA. Only five models  
310 are currently available, and they are for different tectonic environments (i.e., different styles of  
311 faulting; see Section “Overview of PFDHA methodology”), making comparison difficult but  
312 meaningful as shown in later sections of this paper. Inviting new PFDHA model development  
313 teams to participate in this project allows: i) more than a single model for a given kinematic  
314 conditions (e.g., Nurminen et al., 2021 for all dip-slip faults); ii) consideration of new regressions  
315 made for specific components of PFDHA (e.g., Ferrario and Livio, 2021, which revised and  
316 updated the conditional probability of slip for distributed ruptures published by Youngs et al.,  
317 2003); iii) incorporation of the epistemic uncertainty with logic trees and its exploration with  
318 tornado plots that will be provided by each team; and iv) verifications phase to ensure published  
319 PFDHA models are implemented correctly in computer codes.

320         An IAEA TECDOC will be developed in the final step (Step 3) to assist Member States  
321 with conducting PFDHA at existing and/or new nuclear installations. The TECDOC will contain:  
322 i) updated information about the main components of PFDHA, such as the conditional probability  
323 of slip given a magnitude and the conditional probability of exceedance for a given value of  
324 displacement on principal fault; ii) results of the benchmarking of all available models for two

325 example sites in different environments and with different levels of seismic activity; and iii)  
326 guidelines on how to perform the earthquake and/or displacement approach considering all  
327 potential geological information available. The new TECDOC, which will be considered the final  
328 product of this project, aspires to deliver technical guidance on performing PFDHA that is not  
329 currently available in the existing documents and guidelines in the nuclear industry professional  
330 literature.

331

### 332 *Base case and sensitivity cases*

333

334 Step 1 includes a base case and four sensitivity cases to explore differences in seismic  
335 source parametrization and fault-to-site distance. The site dimension ( $z$ ) is the same for the base  
336 and sensitivity cases: 100 x 100 m<sup>2</sup>. The site is in the city of Kumamoto, Japan, near the Futagawa  
337 and the Hinagu fault systems (Fig. 3). The area was recently struck by a large right-lateral strike-  
338 slip earthquake ( $M_w$  7.1, April 16, 2016; Shirahama et al., 2016) that ruptured the Futagawa fault  
339 and the northern tip of the Takano-Shirahata fault, as well as other conjugate fault planes like the  
340 Suizenji fault plane (Fig. 3). For our study herein, we considered only the Futagawa fault system  
341 and the Suizenji fault in seismic source parameterization. The Hinagu fault zone was not  
342 considered due to the large distance between the faults and the selected site.

343 Table 2 summarizes the base and sensitivity case spatial parameters, and Fig. 3b shows a  
344 map configuration of the cases. Deterministic seismic source characterization parameters for the  
345 fault systems are listed in Table 3, and all modelers used this characterization. A source logic tree  
346 with alternative branches for magnitude and mean occurrence rates is provided in Fig. 4. The  
347 magnitude uncertainty in the logic tree (Fig. 4) reflects a factor of 2 in seismic moment per event

348 for each source, and the mean occurrence rate uncertainty is a factor of 3 around the middle branch.  
349 All modelers used the earthquake approach in their PFDHA calculations. The base case and the  
350 four sensitivity cases used here in Step 1 will also be used by other teams in Step 2. Furthermore,  
351 Step 2 will also include second site (location to be determined).

352 The base case hazard is from distributed faulting from a combination of three  
353 approximately located faults in Futagawa fault system (Futagawa, Uto, and Uto Hanto North  
354 faults), and the closest fault-to-site distance ( $r$ ) is 5.2 km (Fig. 3 and Table 2). Four sensitivity  
355 cases were used to explore sensitivity of hazard to type of faulting (i.e., principal or distributed),  
356 magnitude,  $l/L$ , and  $r$ . The first sensitivity case also considers hazard from distributed faulting. In  
357 Sensitivity Case 1, the closest distance  $r$  is 0.6 km because the Suizenji fault (Fig. 3) is treated as  
358 a principal fault source, the map accuracy is inferred, and epistemic uncertainty in source  
359 parameters is not included (i.e., only the single-branch case for the Suizenji fault parameters in  
360 Table 3 were used). For the second and third sensitivity cases, the site was assumed to be on a  
361 principal fault, so the closest distance  $r$  is zero and the hazard is from principal faulting. The fourth  
362 sensitivity case is similar to the base case except fault distance  $r$  is 10 km (Fig. 3).

363 The source parameter characterization for the Futagawa fault system (Table 3) was  
364 provided by the IAEA and based on the source characterization by the Headquarters for  
365 Earthquakes Research Promotion (HERP, 2016). To evaluate moment magnitude ( $M_w$ ) and the  
366 occurrence rates, the fault length is determined by the Geological Survey of Japan. The total length  
367 of each scenario is then obtained as the summed lengths of the included faults (i.e., Futagawa, Uto,  
368 and/or Uto-Hanto-North, Fig. 3). Then, earthquake magnitude ( $M_j$ ) is computed by the Japanese  
369 Meteorological agency from the total fault length using the Japanese scaling rule (Matsuda, 1975),  
370 and  $M_j$  is converted to  $M_w$  according to Takemura (1990).  $M_w$  is then used to compute the seismic

371 moment (Kanamori, 1977) and fault area by the characteristic source scaling (Irikura and Miyake,  
372 2001). Other geometrical parameters, such as dip angle and seismogenic thickness, are inferred.  
373 To evaluate the occurrence rate of each scenario, the dislocation is evaluated (per event), as  
374 computed by the Japanese scaling rule between fault length and dislocation (Matsuda et al., 1980).  
375 Then, the average recurrence interval is calculated based on average slip rate and dislocation (per  
376 event), with the average slip rate determined from geomorphological survey results (HERP, 2016).

377 The same procedure was followed for the Suizenji fault. Because this fault was not  
378 identified by HERP (2016) before the 2016 Kumamoto earthquake, we use fault length and  
379 geomorphological survey results published by Goto et al. (2017) to compute the Suizenji fault  $M_w$   
380 and mean occurrence rate (Table 3).

381

### 382 *Step 1 results*

383

384 Figure 5 shows the results for the base case and four sensitivity cases (Table 2) as  
385 displacement hazard curves. The hazard curves are expressed in terms of annual frequency of  
386 exceedance (AFOE,  $\text{yr}^{-1}$ ) versus displacement (cm), and curves on Fig. 5 are for distributed  
387 displacement (Figs. 5a, 5b, 5c, and 5f) and for principal faulting (Figs. 5d to 5e). Epistemic  
388 uncertainty in the parameters listed in Table 3 was included only in Figure 5b. For the base case,  
389 the results represent the total hazard curve given by the sum of contributions from all Futagawa  
390 fault system scenarios considered (Fig. 3). For principal displacement, the models use conditional  
391 probabilities of slip given a magnitude and expected displacement given the location of the site  
392 along the fault. Distributed displacement is determined from a conditional probability of slip at

393 distance  $r$  from the rupture, given a magnitude and expected displacement for the site location  
394 away from the fault.

395 The Youngs et al. (2003) model produces the highest distributed displacement hazard in  
396 the base case and sensitivity case 4, and the Nurminen et al. (2020) model produces the lowest  
397 hazard (Figs. 5a and 5f). All models show the same behaviour: hazard curves are flat curve in  
398 between 0.01 cm and 10 cm, and the slopes of the curves increase as AFOE decreases and  
399 displacement increases. The Nurminen et al. (2020) model produces the highest hazard in  
400 sensitivity case 1 (Fig. 5b). The Takao model hazard is slightly lower in sensitivity case 1 (relative  
401 to the base case), and the Petersen and Youngs model hazards are slightly higher. Because the  
402 mean occurrence rate for the base case (i.e., the sum of mean rate of four scenarios of the Futagawa  
403 fault system, Table 3) is similar to that of sensitivity case 1 (Suizenji fault only, Table 3), the  
404 differences in hazard curves are probably related to different conditional probabilities used by each  
405 model. Sensitivity case 1 hazard curves from the Petersen, Takao, and Youngs models are all  
406 shifted slightly to the left compared to the base case (by about one order of AFOE magnitude).  
407 This indicates that in the Petersen, Takao, and Youngs models, the change in the conditional  
408 probability of distributed faulting with distance,  $r$ , has less of an impact than the maximum  
409 magnitude. However, the fault-to-site distance  $r$  is the controlling parameter in the Nurminen et  
410 al. (2020) model: base case distance is 5.2 km, and the distance in the first sensitivity case is 0.6  
411 km. This change yields an AFOE that is almost six orders of magnitude higher in the sensitivity  
412 case 1 than in the base case.

413 Figure 5b shows mean displacement hazard curves and 90% confidence intervals, for the  
414 base case, considering epistemic uncertainty in source characterization (Fig. 4). For all models, the  
415 90% confidence interval is always within about one order of AFOE magnitude. While the

416 epistemic uncertainty in source parameters ( $M_w$  and occurrence rate) is important for PFDHA,  
417 more significant differences are observed between different models (and therefore among different  
418 kinematic styles) (Fig. 5b).

419 Figures 5d and 5e show sensitivity cases 2 and 3, which are related to principal faulting. In  
420 both cases and for all models, the hazard is about two orders of AFOE magnitude higher compared  
421 to the base case (Fig. 5a), where the site is 5.2 km far from the principal fault. In the sensitivity  
422 case 2 (Fig. 5d) the hazard is higher than the third sensitivity case for all models and this is mainly  
423 due to the difference in the  $M_w$  between the two cases (Table 2 and 3). However, the impact of this  
424 difference is much evidence for the Takao and Moss than the Youngs and Petersen models. This  
425 means that the conditional probability of slip and the conditional probability of exceedance (Eq.  
426 5) for Takao and Moss models are more  $M_w$  sensitive than the Youngs and Petersen models.

427

## 428 DISCUSSION

429

430 The results of Step 1 (Fig. 5) highlight the importance of source parametrization in terms  
431 of maximum magnitudes, occurrence rates, and style of faulting when a PFDHA is performed. The  
432 results also reveal significant differences in the hazards calculated for different displacement  
433 models, which are based on fault kinematics and tectonic environment. Strike slip, reverse, and  
434 normal events have different stress regimes which, for a given magnitude, appear to yield different  
435 displacements along the principal fault and probabilities of surface rupture. This is illustrated in  
436 Figure 6, where probabilities of distributed surface rupture from the different models used in Step  
437 1 are shown. For example, the difference in rupture probabilities between the Youngs and Takao  
438 models for the base case ( $r = 5.2$  km, Fig. 6) is roughly two orders of magnitude, resulting in the

439 same spread the displacement hazard curves (Fig. 5a). For sensitivity case 1 ( $r = 0.6$  km, Fig. 6),  
440 the difference between the Petersen and Youngs models is less than an order of magnitude, and a  
441 similar spread is also reflected in the displacement hazard curves (Fig. 5c).

442 Each PFDHA model used in Step 1 is based on conditional rupture probabilities developed  
443 for different tectonic regimes using independent databases. Hence, differences in Figure 6 are not  
444 surprising. Each model is also developed following different assumptions. For example, the  
445 Petersen and Nurminen models do not consider triggered ruptures and are not recommended for  
446 distances greater than two or three kilometres. In contrast, the Youngs model for distributed  
447 ruptures was developed from a more spatially extensive database, providing assessments of rupture  
448 probabilities for distances up to 20 km. While it is important to select the appropriate model for a  
449 given tectonic environment, it is also necessary to understand how to correctly apply these models.  
450 Are the Nurminen and Petersen models suitable for a nuclear installation located at five kilometres  
451 from a capable fault? What site-specific data and knowledge are needed to correctly apply a given  
452 model? Answers to these questions are what the Member States expect from the TECDOC, which  
453 will be published at the end of this project. It is anticipated that the TECDOC will allow the  
454 Member States to better understand PFDHA and alternative models that can be applied.

455 Scarceness of data is another important point to keep in mind when performing PFDHA.  
456 The available datasets used PFDHA model development are limited compared to ground motion  
457 datasets used in probabilistic seismic hazard analysis model development. Existing datasets often  
458 lack details about the complexity of surface faulting and commonly include only seismological  
459 information such as earthquake magnitude, focal mechanism and hypocentral depth. To date,  
460 PFDHA model developers have relied on their own data compilations specific to the local tectonic  
461 regime of the area been investigated (e.g., Nurminen et al., 2020) or published datasets containing

462 information of primary or secondary ruptures. For example, Youngs et al. (2003) used Wells and  
463 Coppersmith (1993) for conditional probability of principal surface rupture and Pezzopane and  
464 Dawson (1996) to assess conditional probability for distributed rupture. Petersen et al. (2011)  
465 collected additional data for both principal and distributed ruptures. In the last few years, efforts  
466 have been made toward a worldwide and unified database of surface rupture for fault displacement  
467 hazard assessment. The SURE database (Baize et al., 2020) contains surface rupture information  
468 and fault displacement data for 45 earthquakes with magnitude ranging from 5.0 to 9.0 and a total  
469 of 15,000 observed coseismic surface displacement measurements and 56,000 mapped rupture  
470 segments. The database includes geo-referenced GIS files of surface ruptures and three tables  
471 summarizing pertinent displacement and rupture observations and earthquake information. The  
472 next step towards developing a robust surface rupture dataset is utilizing a combination of  
473 traditional field mapping with remote sensing techniques. Recent advances in remote-sensing  
474 analysis (e.g., Monterroso et al., 2020) allow sampling of both principal and distributed rupture  
475 and displacement uniformly and systematically, improving statistical results and data coverage and  
476 precision. Moreover, these tools allow one to collect information on coseismic deformation in  
477 remote or inaccessible areas and provide broad spatial coverage, improving data collection for  
478 large magnitude ruptures. Finally, new remote sensing techniques also afford better differentiation  
479 of primary and secondary ruptures in moderate-to-small magnitude earthquakes (e.g., Ritz et al.,  
480 2020).

481         There are a lot of other issues in PFDHA that worth mentioning. For example, a key  
482 challenge in developing PFDHA databases and models is classifying faults and related  
483 displacements as primary or secondary. It is extremely important, to reduce epistemic uncertainty  
484 related to primary fault location, have a well-known and mapped principle fault trace and it is also



485 important have a good record of distributed ruptures to better constraint the conditional probability  
486 of having distributed ruptures far from the principal fault. Therefore, more precise definition and  
487 classification methods are needed, for example, categorizing the distributed ruptures (e.g., only  
488 sympathetic, or only triggered ruptures) and applying a different regression for a different kind of  
489 distributed rupture. Another issue is the soil condition. In general, nuclear installations are or will  
490 be located where geological conditions are acceptable (i.e., rock). Soil sites may also be selected  
491 if bearing capacity is sufficient (IAEA, 2005). Soil conditions may play a role in PFDHA. Moss  
492 et al. (2013) show that the stiffness of the upper thirty meters of geologic material has a strong  
493 impact on rupture propagation from depth to the ground surface in reverse environment. Bray et  
494 al. (1994) argues that the characteristics of the soil overlying the bedrock fault strongly influence  
495 the observed earthquake fault rupture propagation behaviour. All models used in this  
496 benchmarking exercise do not consider the condition of secondary rupture sites. It is expected that  
497 soil effects will be considered in future studies for other tectonic environments. Finally, existing  
498 models were developed primarily using empirical approaches. It is expected that the advancement  
499 of 3-D physics-based numerical simulations (e.g., Dalguer et al., 2020) will complement empirical  
500 models. In particular, dynamic rupture approaches can be useful in the case where regressions for  
501 distributed ruptures need to be extrapolated to large rupture distances (e.g. the models of Nurminen  
502 et al. 2020 and Petersen et al. 2011 for distances greater than 2 to 3 km).

503

504

## CONCLUSIONS

505

506

507

The IAEA recommends PFDHA as a tool to evaluate the impact of capable faults in the vicinity of an existing or planned nuclear installation. Because there is lack of documented case

508 histories on PFDHA in the scientific and engineering literature, particularly compared to PSHA  
509 for ground motion hazard assessment, the Member States requested that the IAEA document a  
510 recommended approach and evaluation of available alternative parameterizations in the literature  
511 to better understand hazard results. To meet this request, the IAEA initiated the PFDHA  
512 Benchmarking Project.

513         The PFDHA Benchmarking project consists of three steps: 1) example applications to  
514 identify the most important aspects in the PFDHA models, 2) detailed analyses for understanding  
515 of model differences, and 3) development of a TECDOC to provide specific guidelines for PFDHA  
516 application. The project commenced in November 2020. Step 1 has been completed and is  
517 described in this paper. The results of Step 1 allow us to draw important preliminary conclusions,  
518 which will help in directing additional analyses in Step 2 and the contents of the TECDOC. It is  
519 shown, through the evaluation of epistemic uncertainty in source characterization and comparison  
520 among different models and their rupture probabilities (Figs. 5 and 6), that choosing appropriate  
521 models and correct model applications are important for any existing or new nuclear installations.  
522 Comparisons among different models that reflect different fault types or regional tectonic  
523 characteristics, performed during Step 1, will be useful for the Member States to better understand  
524 how each model is built and how to correctly apply it. The IAEA will invite other PFDHA  
525 modelling teams to participate in Step 2 to analyse two example sites in different tectonic  
526 environment, which will allow verification of model implementation and the comparison of hazard  
527 results for a given tectonic regime. The IAEA TECDOC will be delivered at the end of Step 3,  
528 which will assist the Member States in performing PFDHA and contribute to international nuclear  
529 safety.

530

531  
532  
533  
534  
535  
536  
537  
538  
539  
540  
541  
542  
543  
544  
545  
546  
547  
548  
549  
550  
551

## **DATA AND RESOURCES**

The source parameters used to compute the hazard curves in Figure 5 are listed in Table 3. The PFDHA approaches used are described within the papers cited in the References.

## **DECLARATION OF COMPETING INTERESTS**

The authors acknowledge there are no conflicts of interest recorded.

## **ACKNOWLEDGMENTS**

We want warmly to thank the Associate Editor L. A. Dalguer, A. Hatem, N. Luco, and two anonymous reviewers for their useful comments and suggestions that improved the manuscript. Great appreciation is extended to Prof. P. Boncio, Prof. Bruno Pace, Dr. Oona Scotti, Dr. Stéphane Baize and Dr. Fiia Nurminen for the fruitful discussion during our meeting. We also want to thank Dr. A. Suzuki for contributing to the drafting work as an intern of IAEA. Any use of trade, firm, or product names is for descriptive purposes only and does not imply endorsement by the U.S. Government.

## **REFERENCES**

552 American Nuclear Society Standards Committee Working Group ANS-2.30 (2015). Criteria for  
553 Assessing Tectonic Surface Fault Rupture and Deformation at Nuclear Facilities, ANSI/ANS-  
554 2.30-2015.

555 Baize, S., F. Nurminen, A. Sarmiento, T. Dawson, M. Takao, O. Scotti, T. Azuma, P. Boncio, J.  
556 Champenois, F. R. Cinti., R. Civico, C. Costa, L. Guerrieri, E. Marti, J. McCalpin, K.  
557 Okumura, and P. Villamor (2020). A worldwide and unified database of surface ruptures  
558 (SURE) for fault displacement hazard analyses, *Seismol. Res. Lett.* **91(1)** 499-520, doi:  
559 10.1785/0220190144.

560 Bray, J. D., R. B. Seed, L. S. Cluff, and H. B. Seed (1994). Earthquake fault rupture propagation  
561 through soil. *J. Geotech. Eng.*, **120** (3), 543-561.

562 Coppersmith, K. J., and R.R. Youngs (2000). Data needs for probabilistic fault displacement  
563 hazard analysis, *J. Geodyn.*, **29(3-5)**, 329-343, [https://doi.org/10.1016/S0264-3707\(99\)00047-](https://doi.org/10.1016/S0264-3707(99)00047-2)  
564 2.

565 Cornell, C.A. (1968). Engineering seismic risk analysis, *Bull. Seismol. Soc. Am.*, **58(5)**, 1583-1606.

566 Dalguer, L.A., H. Wu, Y. Matsumoto, K. Irikura, T. Takahama, and M. Tonagi (2020).  
567 Development of Dynamic Asperity Models to Predict Surface Fault Displacement Caused by  
568 Earthquakes, *Pure Appl. Geophys.* **177(5)**, 1983-2006, DOI: 10.1007/s00024-019-02255-8.

569 Ferrario, M. F. and F. Livio (2021). Conditional probability of distributed surface rupturing during  
570 normal-faulting earthquakes, *Solid Earth*, **12**, 1197-1209, [https://doi.org/10.5194/se-12-1197-](https://doi.org/10.5194/se-12-1197-2021)  
571 2021.

572 Goto, H., H. Tsutsumi, S. Toda, and Y. Kumahara (2017). Geomorphic features of surface ruptures  
573 associated with the 2016 Kumamoto earthquake in and around the downtown of Kumamoto

574 City, and implications on triggered slip along active faults, *Earth, Planets and Space*, **69**, 26,  
575 <https://doi.org/10.1186/s40623-017-0603-9>.

576 Headquarters for Earthquake Research Promotion (2016). Evaluation of the Futagawa and Hinagu  
577 Fault Zones. Available at: [http://www.jishin.go.jp/main/chousa/13feb\\_chi\\_kyushu/k\\_11.pdf](http://www.jishin.go.jp/main/chousa/13feb_chi_kyushu/k_11.pdf)  
578 [accessed May 25, 2021].

579 International Atomic Energy Agency (IAEA) (2005). Geotechnical Aspects of Site Evaluation and  
580 Foundations for Nuclear Power Plants, IAEA Safety Standards Series No. NS-G-3.6, Vienna.

581 International Atomic Energy Agency (IAEA) (2006). Fundamental Safety Principles, IAEA Safety  
582 Standards Series No. SF-1, IAEA, Vienna.

583 International Atomic Energy Agency (IAEA) (2010). Seismic Hazards in Site Evaluation for  
584 Nuclear Installations, *IAEA Safety Standards Series*, Specific Safety Guide, SSG-9, IAEA,  
585 Vienna.

586 International Atomic Energy Agency (IAEA) (2019). Site Evaluation for Nuclear Installations,  
587 IAEA Safety Standards Series No. SSR-1, IAEA, Vienna.

588 International Atomic Energy Agency (IAEA) (2021a). Seismic Hazards in Site Evaluation for  
589 Nuclear Installations No. DS507, Revision of Safety Guide SSG-9, IAEA, Vienna (in  
590 publication).

591 International Atomic Energy Agency (IAEA) (2021b). An Introduction to Probabilistic Fault  
592 Displacement Hazard Analysis in Site Evaluation for Existing Nuclear Installations, IAEA  
593 TECDOC, Vienna (in publication).

594 Irikura, K., and H. Miyake (2001). Prediction of strong ground motions for scenario earthquakes,  
595 *Journal of Geography (in Japanese)*, **110(6)**, 849-875.

596 Kanamori, H. (1977). The energy release in great earthquakes, *J. Geophys. Res.*, **82(20)**, 2981-  
597 2987, <https://doi.org/10.1029/JB082i020p02981>.

598 Lavrentiadis G., N. Abrahamson (2019). Generation of Surface- Slip Profiles in the Wavenumber  
599 Domain, *Bull. Seismol. Soc. Am.*, **109** (3), 888–907, doi: <https://doi.org/10.1785/0120180252>.

600 Matsuda, T. (1975). Magnitude and recurrence interval of earthquakes from a fault, *J. Seism. Soc.*  
601 *Japan, Series 2*, **28**, 269-284.

602 Matsuda, T., H. Yamazaki, T. Nakata, and T. Imaizumi (1980). Earthquake fault of the Rikuu  
603 earthquake of 1896 (In Japanese), *Bull. Earthq. Res. Inst.*, Univ. Tokyo, **55**, 795-855.

604 Monterroso, F., M. Bonano, C.D. Luca, R. Lanari, M. Manunta, M. Manzo, G. Onorato, I. Zinno,  
605 and F. Casu (2020). A Global Archive of Coseismic DInSAR Products Obtained Through  
606 Unsupervised Sentinel-1 Data Processing, *Rem. Sens.*, **12**, 3189.

607 Moss, R. E. S., and Z. E. Ross (2011). Probabilistic fault displacement hazard analysis for reverse  
608 faults, *Bull. Seismol. Soc. Am.*, **101(4)**, 1542-1553.

609 Moss, R.E.S., K.V Stanton, and M.I. Buelna (2013). The Impact of Material Stiffness on the  
610 Likelihood of Fault Rupture Propagating to the Ground Surface, *Seismol. Res. Lett.*, **84(3)**,  
611 485.

612 Nurminen, F., P. Boncio, F. Visini, B. Pace, A. Valentini, S. Baize S., and O. Scotti (2020).  
613 Probability of occurrence and displacement regression of distributed surface rupturing for  
614 reverse earthquakes, *Frontiers in Earth Science*, doi: 10.3389/feart.2020.581605.

615 Nurminen, F., F. Visini, S. Baize, P. Boncio, B. Pace, O. Scotti, and A. Valentini (2021).  
616 Probability of distributed surface rupturing occurrence and displacement regression for dip-  
617 slip earthquakes, EGU General Assembly 2021, online, 19–30 Apr 2021, EGU21-12792,  
618 <https://doi.org/10.5194/egusphere-egu21-12792>, 2021.

619 Petersen, M. D., T. E. Dawson, R. Chen, T. Cao, C. J. Wills, D. P. Schwartz, and A. D. Frankel  
620 (2011). Fault displacement hazard for strike-slip faults, *Bull. Seismol. Soc. Am.*, **101**(2), 805-  
621 825, doi: 10.1785/0120100035.

622 Pezzopane, S. K. and T. E. Dawson (1996). Fault displacement hazard: A summary of issues and  
623 information, in *Seismotectonic Framework and Characterization of Faulting at Yucca*  
624 *Mountain, Nevada, U.S. Geological Survey Administrative Report prepared for the U.S.*  
625 *Department of Energy*, Chapter 9, 160 pp.

626 Ritz, J. F., S. Baize, M. Ferry, C. Larroque, L. Audin, B. Delouis and E. Mathot (2020). Surface  
627 rupture and shallow fault reactivation during the 2019 Mw 4.9 Le Teil earthquake, France.  
628 *Commun. Earth Environ.*, **1**, 10, <https://doi.org/10.1038/s43247-020-0012-z>.

629 Shirahama, Y., Mori, H., Maruyama, T., and M. Yoshimi (2016). Geological Survey of Japan  
630 AIST Emergency Survey Report. Available at: <http://g-ever.org/updates/?p=334> [accessed at  
631 May 5, 2021].

632 Stepp, J.C., I. Wong, J. Whitney, R. Quittmeyer, N. A. Abrahamson, N.A., G. Toro, R. Youngs,  
633 K. Coppersmith, J. Savy, and T. Sullivan (2001). Yucca Mountain PSHA Project Members,  
634 2001. Probabilistic Seismic Hazard Analyses for Ground Motions and Fault Displacement at  
635 Yucca Mountain, Nevada, *Earthquake Spectra*, **17**, p. 113–151, doi: 10.1193/1.1586169.

636 Takao, M., T. Tani, T. Oshima, T. Annaka, and T. Kurita (2016). Maximum Likelihood Estimation  
637 of the Parameters regarding Displacement Evaluation of Distributed Fault in PFDHA, *Journal*  
638 *of the Japanese Association of Earthquake Engineering*, **16**, p. 2\_96–2\_101, doi:  
639 10.5610/jaee.16.2\_96.

640 Takao, M., J. Tsuchiyama, T. Annaka, and T. Kurita (2013). Application of Probabilistic Fault  
641 Displacement Hazard Analysis in Japan, *Journal of the Japanese Association of Earthquake*  
642 *Engineering*, **13**, p. 17–36, doi: 10.5610/jaee.13.17.

643 Takao, M., K. Ueta, T. Annaka, T. Kurita, H. Nakase, T. Kyoya, and J. Kato (2014). Reliability  
644 Improvement of Probabilistic Fault Displacement Hazard Analysis, *Journal of the Japanese*  
645 *Association of Earthquake Engineering*, **14**, p. 2\_16–2\_36, doi: 10.5610/jaee.14.2\_16.

646 Takemura, M. (1990). Magnitude-seismic moment relations for the shallow earthquakes in and  
647 around Japan, *J. Seism. Soc. Japan*, **43**, 257-265.

648 The Standards Committee of the Atomic Energy Society of Japan (2021). A Standard for  
649 Procedure of Fault Displacement Probabilistic Risk Assessment (PRA) for Nuclear Power  
650 Plants, AESJ-SC-P00X:202X, publication process (in Japanese),  
651 [https://www.aesj.net/sc\\_public\\_review/sc-public-110](https://www.aesj.net/sc_public_review/sc-public-110) (last accessed 25 May 2021).

652 United States Nuclear Regulatory Commission (2018). Updated Implementation Guidelines for  
653 SSHAC Hazard Studies, NUREG-2213, USNRC.

654 Wells, D. L., & Coppersmith, K. J. (1993). Likelihood of surface rupture as a function of  
655 magnitude, *Seismol. Res. Lett.*, 64(1), 54.

656 Youngs, R. R., W. J. Arabasz, R. E. Anderson, A. R. Ramelli, J. P. Ake, D. B. Slemmons, J. P.  
657 McCalpin, D. I. Doser, C. J. Fridrich, F. H. Swan, A. M. Rogers, J. C. Yount, L. W. Anderson,  
658 K. D. Smith, R. L. Bruhn, P. L. K. Knuepfer, R. B. Smith, C. M. dePolo, D. W. O’Leary, K.  
659 J. Coppersmith, S. K. Pezzopane, D. P. Schwartz, J. W. Whitney, S. S. Olig, and G. R. Toro  
660 (2003). A methodology for probabilistic fault displacement hazard analysis (PFDHA),  
661 *Earthquake Spectra*, **19(1)**, 191-219, doi: 10.1193/1.1542891.



662 **FULL MAILING ADDRESS FOR EACH AUTHOR**

663 A. Valentini, Y. Fukushima, P. Contri, M. Ono

664 External Events Safety Section, International Atomic Energy Agency, IAEA

665 Vienna International Centre, PO Box 100, 1400 Vienna, Austria

666 [A.Valentini@iaea.org](mailto:A.Valentini@iaea.org), [Y.Fukushima@iaea.org](mailto:Y.Fukushima@iaea.org), [P.Contri@iaea.org](mailto:P.Contri@iaea.org), M.Ono@iaea.org

667

668 T. Annaka

669 Tokyo Electric Power Services Co., Ltd.

670 9F, KDX Toyosu Grandsquare

671 1-7-12, Shinonome, Koto-ku, Tokyo, 135-0062, Japan

672 [annaka@tepsco.co.jp](mailto:annaka@tepsco.co.jp)

673

674 T. Sakai

675 Nuclear Risk Research Center, Central Research Institute of Electric Power Industry

676 1646 Abiko, Abiko-shi, Chiba, 270-1194 Japan

677 [t-sakai@ciepi.denken.or.jp](mailto:t-sakai@ciepi.denken.or.jp)

678

679 R. Chen

680 California Geological Survey

681 801 K Street, MS 12-32, Sacramento, CA 95814

682 [rui.chen@conservation.ca.gov](mailto:rui.chen@conservation.ca.gov)

683

684 F. Visini

685 Istituto Nazionale di Geofisica e Vulcanologia

686 Via Cesare Battisti, 53, 56125 Pisa, Italy

687 [francesco.visini@ingv.it](mailto:francesco.visini@ingv.it)

688

689 S. C. Thompson

690 Lettis Consultants International, Inc.

691 1981 N Broadway, Suite 330, Walnut Creek, CA 94596

692 [thompson@lettisci.com](mailto:thompson@lettisci.com)

693

694 R. R. Youngs

695 Wood Environment & Infrastructure Solutions, Inc.

696 180 Grand Avenue, Suite 1100, Oakland, CA 94612

697 [bob.youngs@woodplc.com](mailto:bob.youngs@woodplc.com)

698

699 M. D. Petersen

700 U.S. Geological Survey

701 1711 Illinois Street, Golden, Colorado 80401

702 [mpetersen@usgs.gov](mailto:mpetersen@usgs.gov)  
703  
704 R. E. S. Moss  
705 Dept. Civil and Environmental Engineering 13-259  
706 California Polytechnic State University  
707 San Luis Obispo, California 93407-0353  
708 [rmoss@calpoluy.edu](mailto:rmoss@calpoluy.edu)  
709  
710 E. Viallet  
711 EDF - Nuclear Engineering and New Build Division  
712 Direction Technique,  
713 19 rue Pierre Bourdeix, 69007 Lyon, France  
714 [emmanuel.viallet@edf.fr](mailto:emmanuel.viallet@edf.fr)

715 **TABLES**

716 Table 1. Summary of IAEA safety requirements and recommendations for the three different cases  
 717 according to SSG-9 and DS507 (IAEA, 2010; IAEA 2021a).

	Case 1	Case 2	Case 3
<b>Location of capable fault</b>	<b>Within Site Area</b>	<b>Within Site Vicinity</b>	<b>Outside of Site Vicinity</b>
<b>New site</b>	Exclusionary	Exclusionary if identified as primary	Discretionary as a candidate site
<b>Existing site</b>	PFDHA is recommended*	PFDHA is recommended*	Continued operation

\* If the identified fault has a potential to affect the foundations of items important to safety of nuclear installations.

718  
719

720 Table 2. Summary of parameters used for base and sensitivity cases. The site dimension is 100 x  
 721 100 m<sup>2</sup> for all cases. For the base case and sensitivity cases 2 and 4 the ratio  $l/L$  ranges from 0.1 to  
 722 0.37 because in these cases the total hazard is given by a combination of the three FFS segments  
 723 (Fig. 3 and 4).  $r$  = fault-to-site distance; FFS = Futagawa fault system; SF = Suizenji fault.

	$r$ (km)	Type of faulting	Site coordinates	Source	$l/L$	Map accuracy
Base case	5.2	Distributed	130.7417 – 32.7899	FFS	0.1 – 0.37	Approximately located
Sensitivity Case 1	0.6	Distributed	130.7417 – 32.7899	SF	0.39	Inferred
Sensitivity Case 2	0	Principal	130.7656 – 32.7474	FFS	0.1 – 0.37	-
Sensitivity Case 3	0	Principal	130.7656 – 32.7474	SF	0.39	-
Sensitivity Case 4	10	Distributed	130.7196 – 32.8288	FFS	0.1 – 0.37	Approximately located

724

725 Table 3. Sources and parameters used for seismic source characterization.

Source	Max Rupture Length (km)	Max Rupture Thickness (km)	Average Dip (°)	Magnitude	Mean Rate of Occurrence ( $\times 10^{-5} \text{ yr}^{-1}$ )
Uto (2)	22	14	60 NW	6.5	18.9
Futagawa (1) + Uto (2)	46	14	68.6 NW	6.9	1.28

Uto (2) + Uto-Hanto-North (3)	54	14	60 NW	7	3.53
Futagawa (1) + Uto (2) + Uto-Hanto-North (3)	78	14	64.6 NW	7.2	1.28
Suizenji	5.4	5	60 SW	5.8	23.30

726

727

728 **LIST OF FIGURE CAPTIONS**

729

730 Figure 1. IAEA document hierarchy. Current Safety Fundamentals are in SF-1 (IAEA, 2006); new  
731 Safety Requirements are in SSR-1 (IAEA, 2019); and revised Safety Guide DS507 (IAEA, 2021a)  
732 addresses seismic hazards, updating Safety Guide SSG-9 (IAEA, 2010).

733

734 Figure 2. Site selection for a new site according to IAEA Safety Guide DS507 (IAEA, 2021a). a)  
735 The primary fault rupture is in the site vicinity (5 km radius), and secondary fault ruptures are  
736 within the site area (1 km<sup>2</sup>). This is an exclusionary criterion, per Table 1, if the primary and  
737 secondary fault rupture effects cannot be compensated for by proven design or engineering  
738 measures. b) The primary fault rupture is outside the site vicinity, while the secondary fault  
739 ruptures are within the site vicinity but outside the site area; this is a discretionary criterion, per  
740 Table 1.

741

742 Figure 3. a) Map of the Futagawa fault system (Futagawa, Uto, and Uto-Hanto-North faults) and  
743 Hinagu fault system (Yatsushiro-Sea, Hinagu, and Takano-Shirahata faults) (modified after HERP,  
744 2016). The green star is the location of the site area selected for Step 1. b) Simplification of  
745 Futagawa fault system and Suizenji fault and site locations for base case and four sensitivity cases.

746

747 Figure 4. Source characterization logic tree used in Step 1 for the Futagawa fault system. The  
748 weight of each branch is shown in square brackets. For each scenario, the magnitude uncertainty  
749 ( $\pm 0.2$ ) reflects a factor of 2 uncertainty in seismic moment per event and the mean rate uncertainty

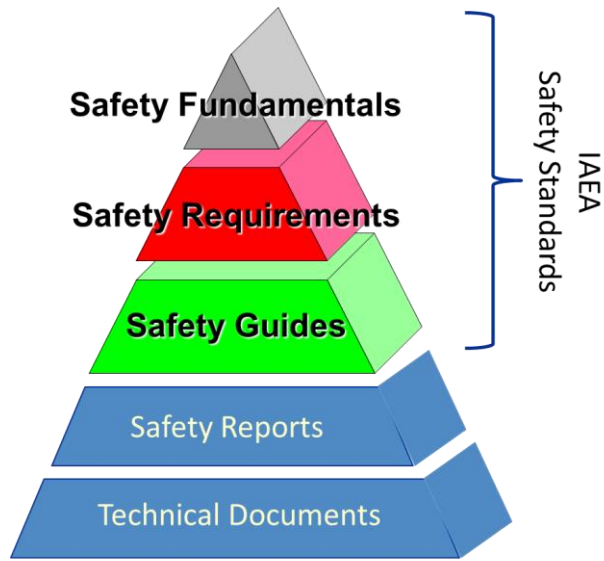
750 is a factor of 3 about the middle branch. The magnitude and mean rate of each scenario are listed  
751 in Table 3.

752

753 Figure 5. Distributed faulting displacement hazard curves in terms of annual frequency of  
754 exceedance (AFOE,  $\text{yr}^{-1}$ ) versus displacement (cm), for base case single path (a) and all sensitivity  
755 cases (c to f). b) Mean displacement hazard curves (solid lines) and 90% confidence intervals  
756 (dashed lines) for base case (distributed faulting) calculated following the logic tree shown in Fig.  
757 3. For the base case, the hazard curves were obtained by summing the contributions of four  
758 different scenarios considered for the Futagawa fault system (Table 3 and Fig. 4). Youngs (Youngs  
759 et al., 2003); Takao (Takao et al., 2013, 2014, 2016); Moss (Moss et al., 2011); Petersen (Petersen  
760 et al., 2011); Nurminen (Nurminen et al., 2020).

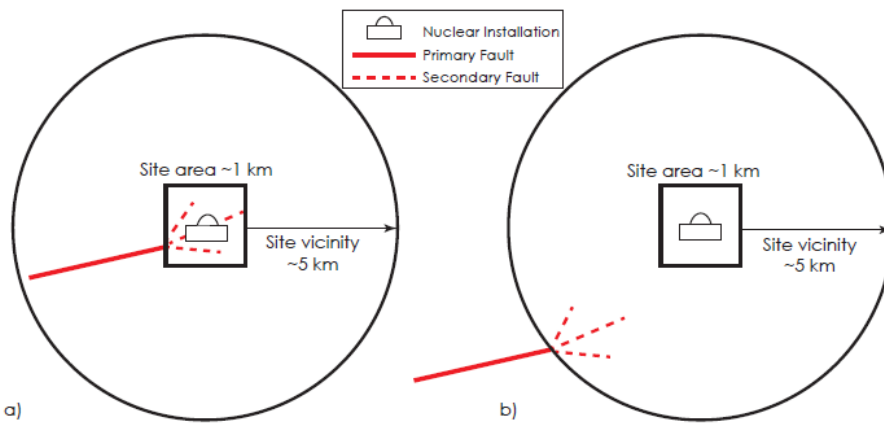
761

762 Figure 6. Conditional probabilities of slip for distributed faulting used by modelers in Step 1.  
763 Youngs and Nurminen probabilities are shown for different magnitudes ( $M$ ) because their  
764 functional form is magnitude-dependent. Petersen and Takao probabilities are not magnitude-  
765 dependent, but they are site-size dependent. In this figure, Petersen and Takao regressions show  
766 probabilities for a site 100 x 100 m. Youngs (Youngs et al., 2003); Takao (Takao et al., 2014);  
767 Nurminen (Nurminen et al., 2020); Petersen (Petersen et al., 2011).



768

769 Figure 1. IAEA document hierarchy. Current Safety Fundamentals are in SF-1 (IAEA, 2006); new  
 770 Safety Requirements are in SSR-1 (IAEA, 2019); and revised Safety Guide DS507 (IAEA, 2021a)  
 771 addresses seismic hazards, updating Safety Guide SSG-9 (IAEA, 2010).

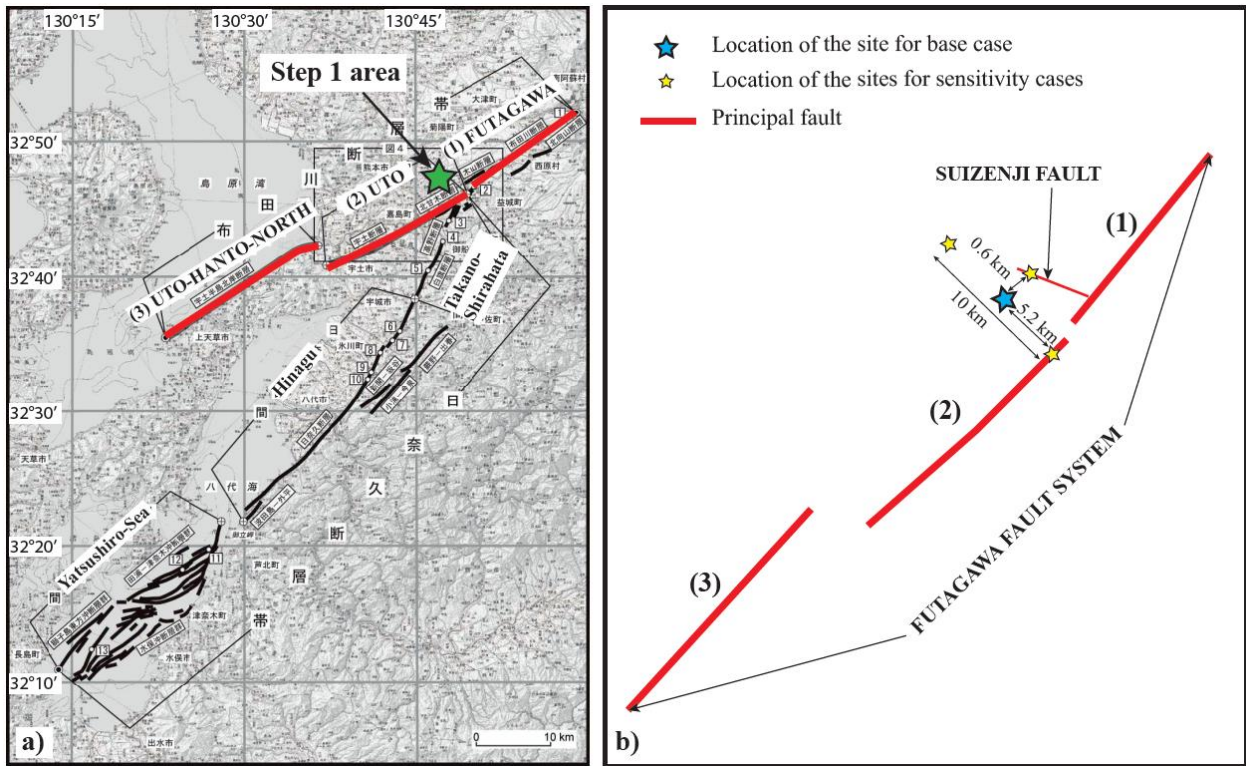


772

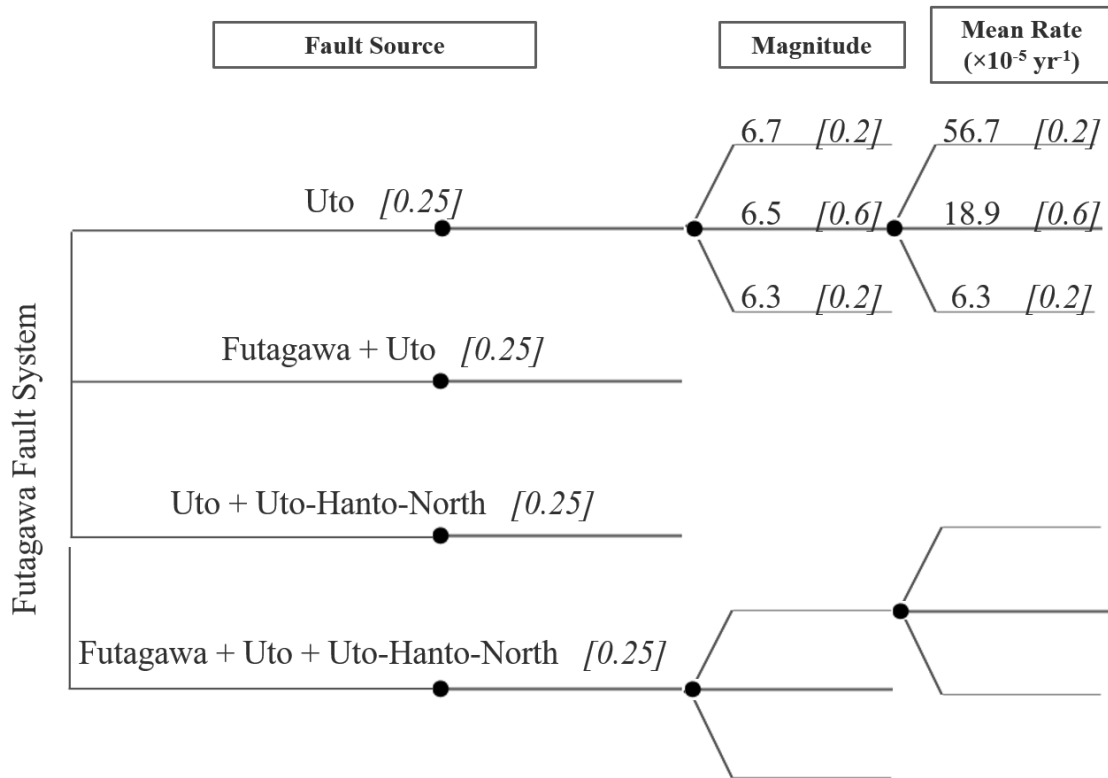
773 Figure 2. Site selection for a new site according to IAEA Safety Guide DS507 (IAEA, 2021a). a)  
 774 The primary fault rupture is in the site vicinity (5 km radius), and secondary fault ruptures are  
 775 within the site area (1 km<sup>2</sup>). This is an exclusionary criterion, per Table 1, if the primary and  
 776 secondary fault rupture effects cannot be compensated for by proven design or engineering  
 777 measures. b) The primary fault rupture is outside the site vicinity, while the secondary fault



778 ruptures are within the site vicinity but outside the site area; this is a discretionary criterion, per  
 779 Table 1.  
 780



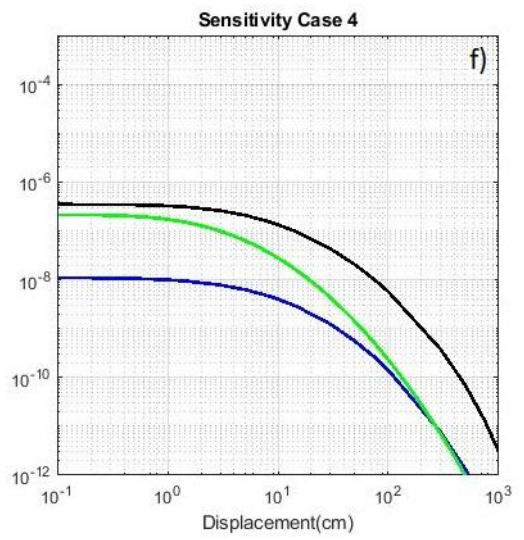
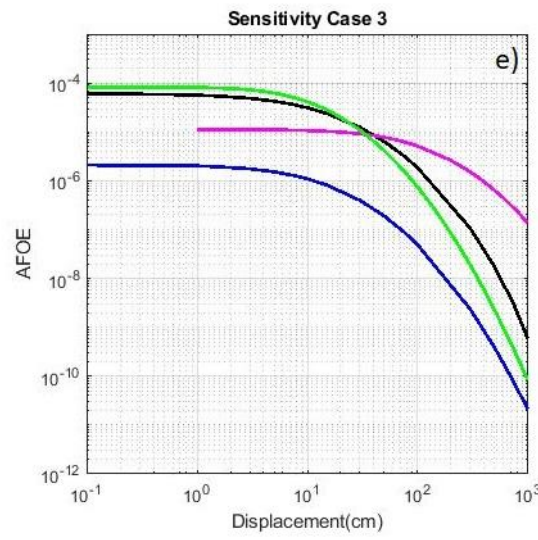
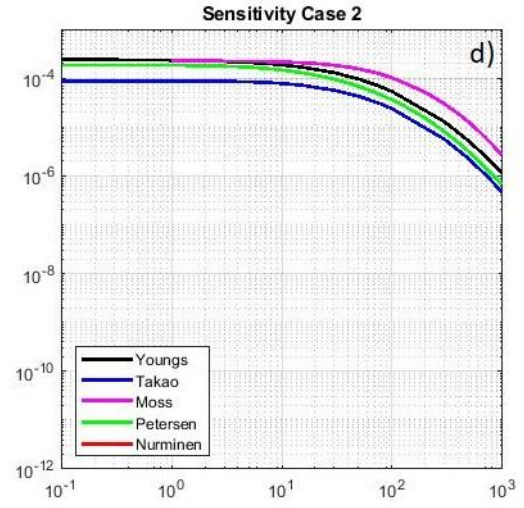
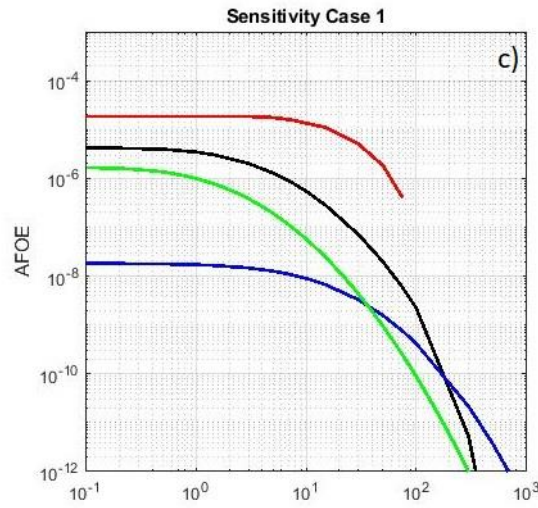
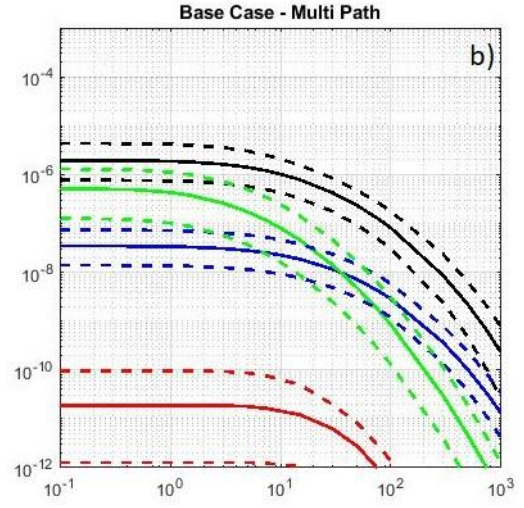
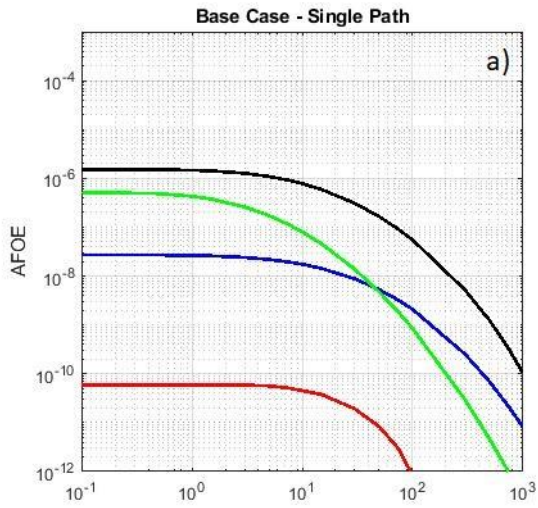
781  
 782 Figure 3. a) Map of the Futagawa fault system (Futagawa, Uto, and Uto-Hanto-North faults) and  
 783 Hinagu fault system (Yatsushiro-Sea, Hinagu, and Takano-Shirahata faults) (modified after HERP,  
 784 2016). The green star is the location of the site area selected for Step 1. b) Simplification of  
 785 Futagawa fault system and Suizenji fault and site locations for base case and four sensitivity cases.



786

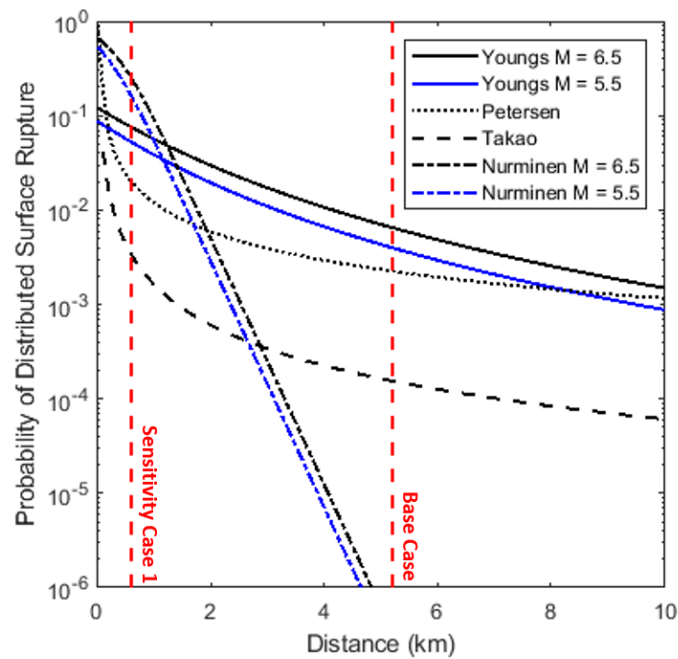
787 Figure 4. Source characterization logic tree used in Step 1 for the Futagawa fault system to capture  
 788 the epistemic uncertainty. The weight of each branch is shown in square brackets. For each  
 789 scenario, the magnitude uncertainty ( $6.5 \pm 0.2$ ) reflects a factor of 2 uncertainty in seismic moment  
 790 per event and the mean rate uncertainty is a factor of 3 about the middle branch. The magnitude  
 791 and mean rate of each scenario are listed in Table 3.

792



794 Figure 5. Distributed faulting displacement hazard curves in terms of annual frequency of  
 795 exceedance (AFOE,  $\text{yr}^{-1}$ ) versus displacement (cm), for base case single path (a) and all sensitivity  
 796 cases (c to f). b) Mean displacement hazard curves (solid lines) and 90% confidence intervals  
 797 (dashed lines) for base case (distributed faulting) calculated following the logic tree shown in Fig.  
 798 3. For the base case, the hazard curves were obtained by summing the contributions of four  
 799 different scenarios considered for the Futagawa fault system (Table 3 and Fig. 4). Youngs (Youngs  
 800 et al., 2003); Takao (Takao et al., 2013, 2014, 2016); Moss (Moss et al., 2011); Petersen (Petersen  
 801 et al., 2011); Nurminen (Nurminen et al., 2020).

802



803

804 Figure 6. Conditional probabilities of slip for distributed faulting used by modelers in Step 1.

805 Youngs and Nurminen probabilities are shown for different magnitudes (M) because their

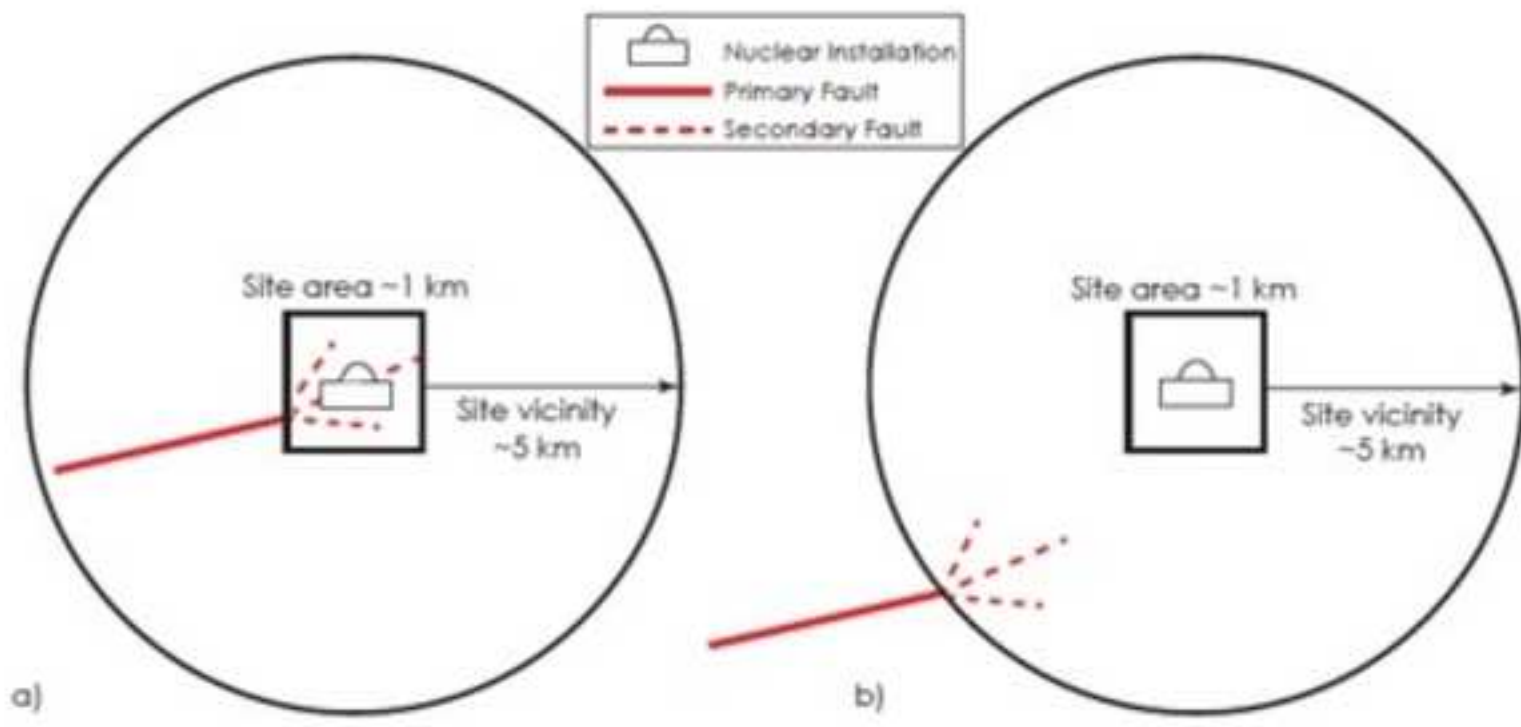
806 functional form is magnitude-dependent. Petersen and Takao probabilities are not magnitude-

807 dependent, but they are site-size dependent. In this figure, Petersen and Takao regressions show

808 probabilities for a site 100 x 100 m. Youngs (Youngs et al., 2003); Takao (Takao et al., 2014);  
809 Nurminen (Nurminen et al., 2020); Petersen (Petersen et al., 2011).







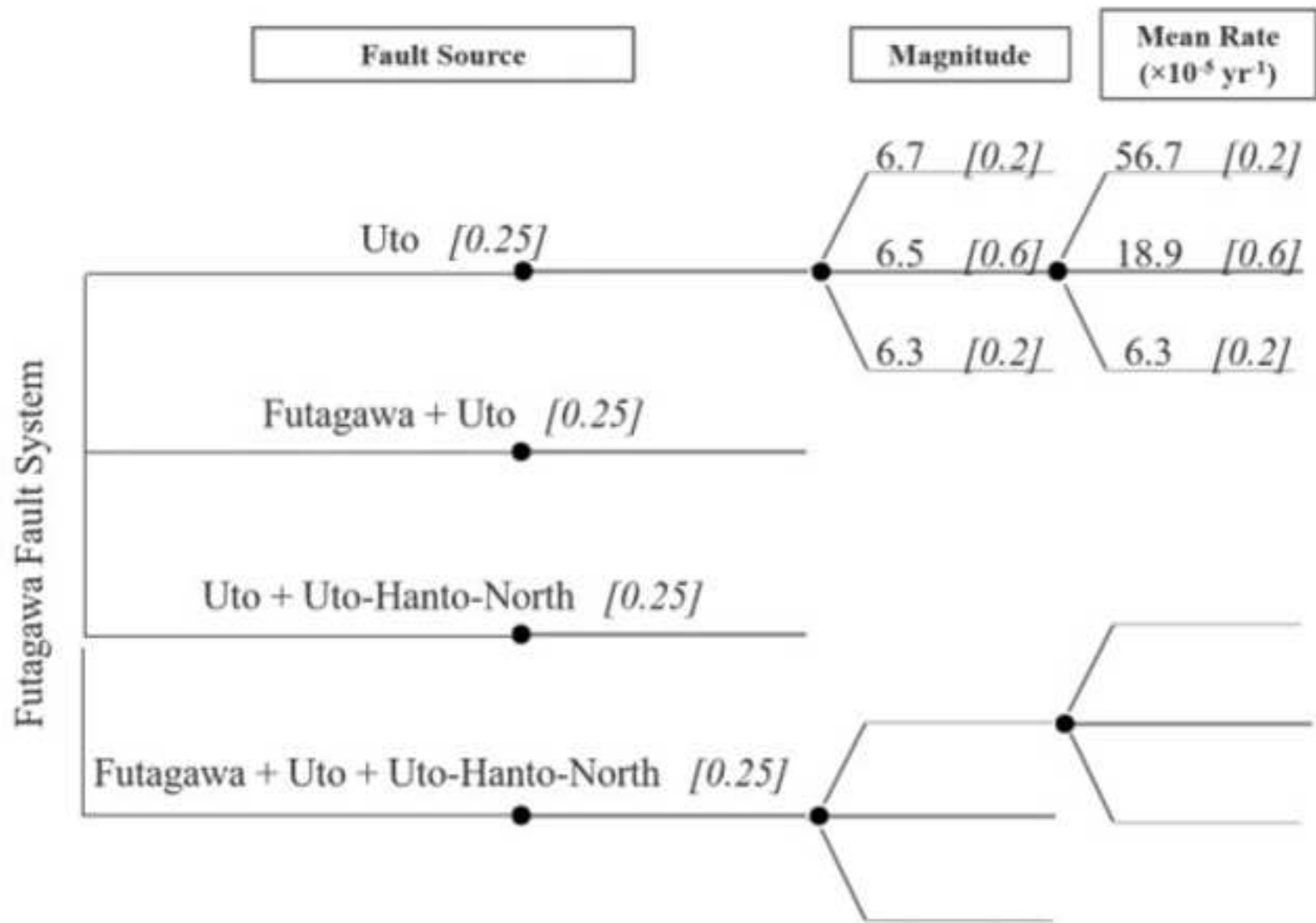




Figure 4

